

An extracellular matrix microarray for probing cellular differentiation

Christopher J Flaim, Shu Chien & Sangeeta N Bhatia

We present an extracellular matrix (ECM) microarray platform for the culture of patterned cells atop combinatorial matrix mixtures. This platform enables the study of differentiation in response to a multitude of microenvironments in parallel. The fabrication process required only access to a standard robotic DNA spotter, off-the-shelf materials and 1,000 times less protein than conventional means of investigating cell-ECM interactions. To demonstrate its utility, we applied this platform to study the effects of 32 different combinations of five extracellular matrix molecules (collagen I, collagen III, collagen IV, laminin and fibronectin) on cellular differentiation in two contexts: maintenance of primary rat hepatocyte phenotype indicated by intracellular albumin staining and differentiation of mouse embryonic stem (ES) cells toward an early hepatic fate, indicated by expression of a β -galactosidase reporter fused to the fetal liver-specific gene, *Ankrd17* (also known as *gtar*). Using this technique, we identified combinations of ECM that synergistically impacted both hepatocyte function and ES cell differentiation. This versatile technique can be easily adapted to other applications, as it is amenable to studying almost any insoluble microenvironmental cue in a combinatorial fashion and is compatible with several cell types.

It is well established that the cellular microenvironment plays a critical role in determining cell fate and function. Extracellular determinants of survival, proliferation, migration and differentiation include soluble signals (cytokines, dissolved gases), insoluble cues (extracellular matrix, cell-cell interactions, biomaterials) and physical stimuli (shear stress). Miniaturization of bioassays using multiwell plates and robotic liquid handling enables combinatorial screening of the effects of soluble species on cellular behavior¹; however, analogous approaches for screening the effects of insoluble cues are in their infancy^{2–4}. Cellular interactions with the ECM are of particular interest, as ligation of an integrin can directly induce cellular signaling, modulate the response to other agonists and influence the behavior of other integrins, a phenomenon called crosstalk^{5,6}. Thus, the extracellular matrix context is likely to be critical in developing an integrated picture of the role of the microenvironment in the fate of many diverse cell types.

Cell-ECM interactions have been studied using several approaches. Typically, purified matrix proteins are adsorbed to cell culture substrates alone or in combination, requiring on the order of 10 μ g of protein per 96-well plate; however, purified matrix for a combinatorial screen can be prohibitively expensive or simply unavailable in sufficient quantity. These two-dimensional approaches are complemented by so-called three-dimensional approaches such as embedding cells within ECM gels^{7,8}. More complex ECM has also been investigated using cell-derived matrix *in vitro*^{9,10} or decellularized tissue sections^{11,12}. In addition to natural ECM components, biomaterials approaches have yielded several hybrid matrices with tethered biomolecules and tunable degradation in a three-dimensional hydrogel context^{13–15}. Thus, with the wealth of interest in cell-ECM interactions, combinatorial techniques for screening of two-dimensional cell-ECM interactions may provide a critical first step towards developing a comprehensive understanding of insoluble cues in the microenvironment.

We sought to adapt robotic spotting technology to develop a robust, accessible method for forming cellular microarrays on combinatorial extracellular matrix domains—a method that required no photolithographic ‘cell micropatterning’ tools or custom-built equipment and only small amounts of protein (~ 10 pg) per experimental condition^{16–19}. With the advent of DNA robotic spotting technology, it is now possible to routinely deliver nanoliter volumes of many different materials, from interfering RNA to peptides to biomaterials, to precise locations on a microarray substrate^{2,4,20–24}. Until now, techniques that use spotted microarrays for cell culture have not been appropriate for experiments such as those conducted in this study because of incompatible process conditions for ECM protein spotting, extensive customization of spotting equipment, or lack of pattern fidelity (that is, cell localization) over time. We overcame these limitations by modifying the protein-printing buffer to allow for ECM deposition with a standard DNA spotter and identifying a microarray substrate that permitted ECM immobilization on a hydrogel surface yet maintained spatially confined cellular islands. Accordingly, we present a method for spotting mixtures of collagen I, collagen III, collagen IV, laminin and fibronectin in 32 combinations with eight replicates per condition on a standard microscope slide using off-the-shelf chemicals and a conventional DNA robotic

Departments of Bioengineering and Medicine, University of California San Diego, 9500 Gilman Drive- MC 0412, La Jolla, California 92093-0412, USA. Correspondence should be addressed to S.N.B. (sbhatia@ucsd.edu).

PUBLISHED ONLINE 21 JANUARY 2005; DOI:10.1038/NMETH736

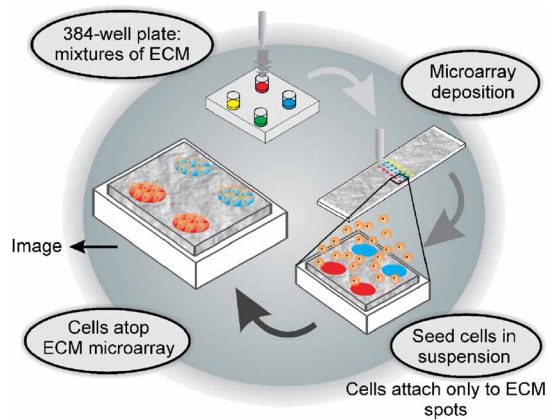


Figure 1 | Schematic depiction of fabrication and use of ECM microarray. Defined ECM mixtures were deposited on a hydrogel slide using a standard DNA microarrayer. Cells were seeded in suspension, cultured for several hours to allow for attachment, and the excess cells were rinsed away. The cell array was then stained for an *in situ* phenotypic marker, imaged and quantified for further analysis.

spotter (Fig. 1). We demonstrated the utility of this approach by application to two different cell types: we assessed the differentiated function of mature, primary rat hepatocytes by albumin immunostaining and differentiation of mouse ES cells along the hepatic lineage as assessed by a β -galactosidase reporter fused to the fetal liver-specific gene, *Ankrd17* (refs. 25,26).

RESULTS

ECM microarray fabrication and characterization

Our design criteria were (i) minimal protein usage, (ii) reproducible fabrication, (iii) low protein carryover, (iv) nonadhesive microarray surface for cells, (v) compatibility with diverse cell types, (vi) ability to maintain cell patterns for about 1 week in serum media and (vii) compatibility with conventional microscopy. We chose a contact deposition-type microarrayer over a piezo dispenser because it can function with as little as 3 μ l of source material. We tested several commercially available microarray surfaces for their ability to confine hepatocytes to collagen I (a model ECM protein) islands for 48 h of culture with 10% serum. Hydrogel (Perkin Elmer), CodeLink (Amersham) and our own

acrylamide slides maintained spatially confined cellular islands for >48 h (Supplementary Fig. 1 online). A wide range of spotting solution concentrations was permissive for cell attachment (see Supplementary Data online).

Next, we verified protein immobilization and assessed whether substantial carryover occurred during the fabrication process. We first characterized the spatial localization of ECM proteins using antigenic recognition (Fig. 2). In each case, high fluorescence corresponded to the expected spatial distribution of the five matrix proteins used. Collagen IV staining showed dim fluorescence in some laminin regions, probably corresponding to a reported 4% cross reactivity of the anti-collagen IV antibody as assessed by radioimmunoassay (Bioscience International). We also spotted alternating test solutions of fluorescein isothiocyanate (FITC)-collagen I and 'buffer only' with the same pin and were unable to detect a signal in 'buffer only' rows using a confocal laser scanner. Thus, we did not detect protein carryover contamination using two separate techniques.

Primary rat hepatocytes adhered preferentially to protein spotted regions and did not attach to the acrylamide gel regions lacking ECM proteins (Fig. 3a,b). The cell patterning was robust over a large surface area (9 \times 9 mm), yielding a uniform array of near confluent cellular islands with a diameter of $150 \pm 5.8 \mu$ m ($n = 15$). Cells were confined to the spotted regions for a period of at least 7 d, after which the most common mode of failure was gel detachment from the slide. Phase-contrast images of the array showed compact cells with polygonal morphology, distinct nuclei and bright intercellular borders consistent with primary hepatocytes (Fig. 3c,d). Cell viability assays, using the fluorescent dyes calcein AM and ethidium homodimer-1, at 24 h and 5 d after plating showed predominantly live cells (~95%) with intact membranes that excluded ethidium homodimer-1 nuclear staining (Fig. 3b).

Effect of ECM composition on hepatocytes and ES cells

To probe primary rat hepatocytes for the effects of ECM composition, cell arrays were stained immunofluorescently for intracellular albumin (a marker of liver-specific function) and analyzed on days 1 and 7. All islands showed similar fluorescent intensity on day 1, with an average of 6.41 ± 0.166 log fluorescent units (two arrays measured). In contrast, day 7 arrays showed notable differences in fluorescent intensity that seemed to be dependent on the initial underlying matrix composition. Quadrants 2 and 3 of the array had

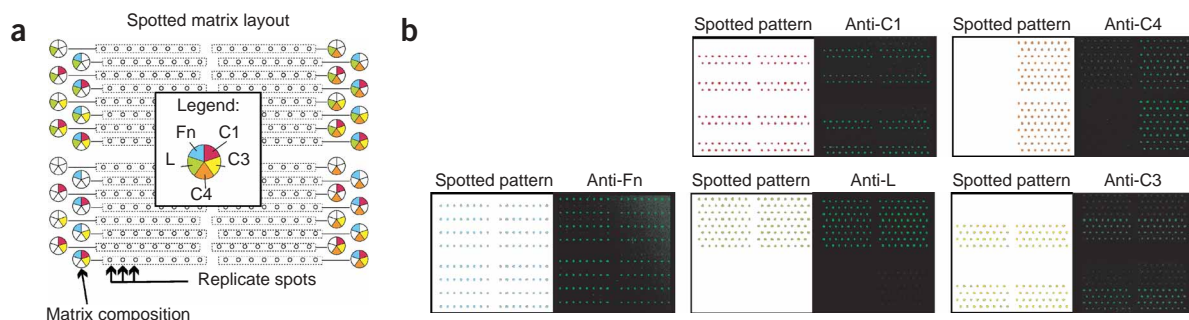


Figure 2 | Characterization of ECM microarray by indirect immunofluorescence. (a) Composition and layout of each row, 32 conditions in eight replicates each. The spotting solution concentration of each ECM molecule, when present in a mixture, was 100 μ g/ml. (b) Correlation of specified array composition and immunofluorescence of replicate arrays demonstrates presence and immunoreactivity of all five ECM components with minimal carryover between conditions. C1, collagen I; C3, collagen III; C4, collagen IV; L, laminin; Fn, fibronectin.

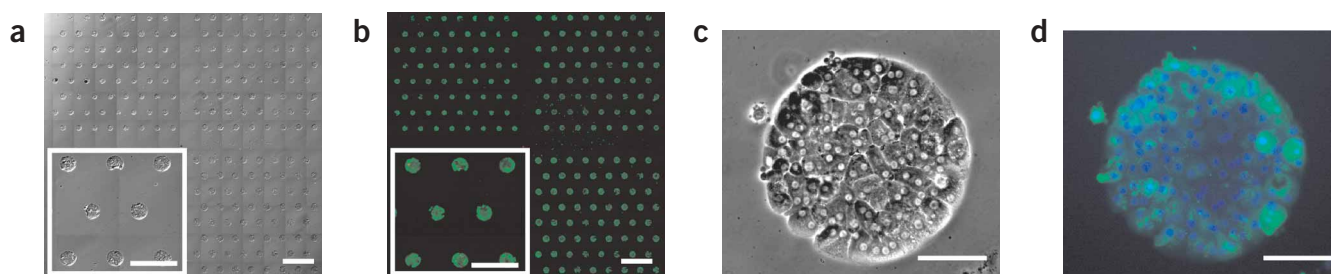


Figure 3 | Primary rat hepatocytes on ECM microarrays. (a) Hoffman contrast montage image of the ECM microarray after 24 h of culture in 10% serum (inset, magnified view). Hepatocytes are well spread, have bright intercellular borders and distinct nuclei, and spread to occupy the full ECM island in all conditions. (b) Live/dead (green/red) staining of hepatocytes using calcein AM and ethidium homodimer-1 reveals ~95% viability at 24 h (inset, magnified view). Scale bars, 1 mm (inset scale bars, 500 μ m). (c,d) High-magnification phase-contrast (c) and fluorescent images (d) of a single island (green, calcein AM; blue, DAPI). Scale bars, 50 μ m.

collagen IV in all spots, and seemed qualitatively and quantitatively to be brighter than quadrants 1 and 4 (Fig. 4a,b). Approximately half of the analyzed mixtures had an albumin signal on day 7 that was greater than the average of day 1 cultures (Fig. 4c). The 15 highest albumin signals are associated with underlying matrices containing collagen IV. In a separate experiment, hepatocytes cultured on serially diluted collagen IV (ranging from 31.2 μ g/ml to 500 μ g/ml) for 5 d showed no significant differences in intracellular albumin signal ($P > 0.05$ for all pairs using one-way ANOVA with a multiple-comparison Tukey post-hoc test, GraphPad Prism software). Taken together, the data suggested that the differences in liver-specific function were not due simply

to a difference in collagen IV concentration but rather to an interaction with other ECM molecules.

Factorial analysis methods were applied to analyze all available day 7 data (four arrays, yielding 1,024 data points) for main effects, 2-, 3- and 4-factor interactions, in addition to the statistical significance of each effect (Fig. 4d). The analysis revealed that the largest overall effect on albumin signal was the increase resulting from collagen IV. Among the other main effects, we found fibronectin also had a positive effect, though to a lesser extent than collagen IV. Laminin and collagen III negatively affected the albumin signal. In agreement with our findings, it has been previously reported that secreted albumin from primary rat

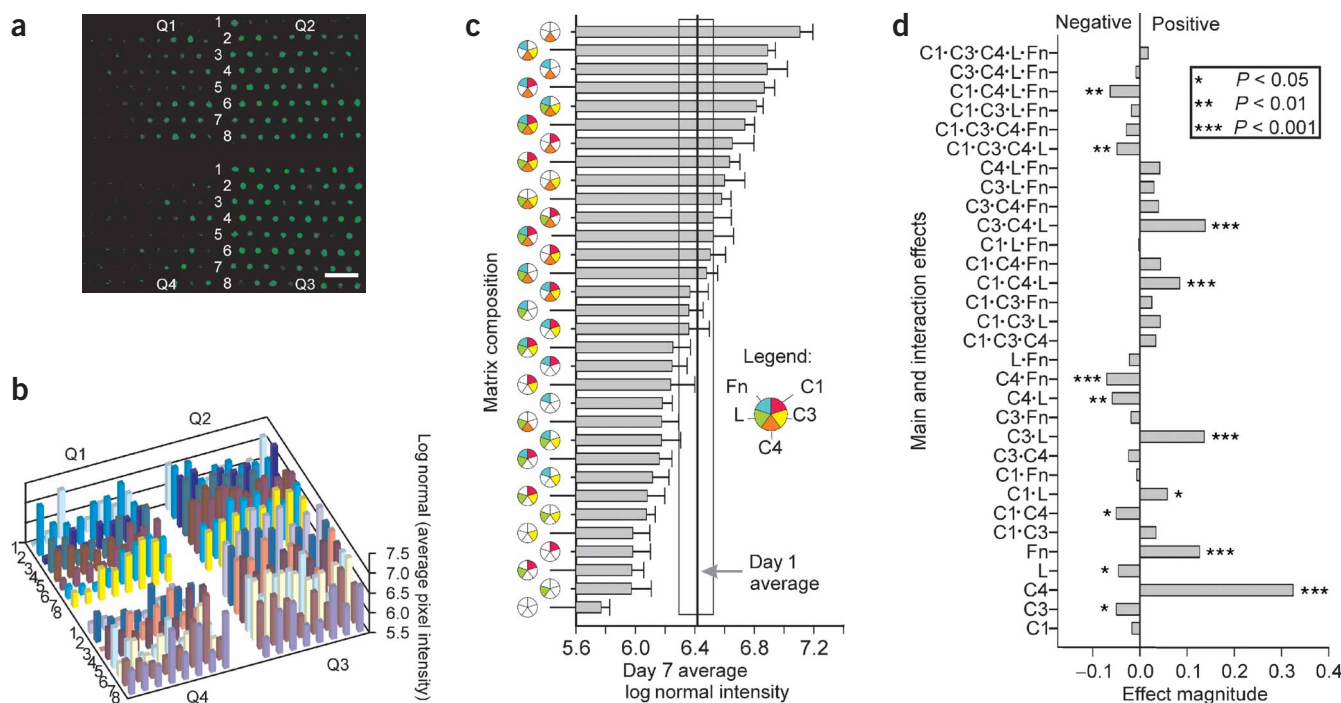


Figure 4 | Cultured hepatocytes show differential intracellular albumin staining in response to matrix composition. (a) Indirect immunofluorescence of intracellular albumin, a marker of differentiated hepatocyte function, on day 7. Note preservation of microarray features after 7 d in 10% serum. (b) Quantification of average pixel intensity per microarray spot in a. (c) Hierarchical depiction of image albumin intensity for each of the matrix mixtures on day 7. Error bars, s.e.m. ($n = 8$). Reference line is the average intensity for hepatocytes on day 1. Error box represents 1 s.d. (d) Results of 2^5 full factorial analysis on intracellular albumin intensity (four microarray data sets). The relative magnitude of main effects as well as 2-, 3-, 4- and 5-factor interactions are shown. Q1, quadrant 1; Q2, quadrant 2; Q3, quadrant 3; Q4, quadrant 4; C1, collagen I; C3, collagen III; C4, collagen IV; L, laminin; Fn, fibronectin.

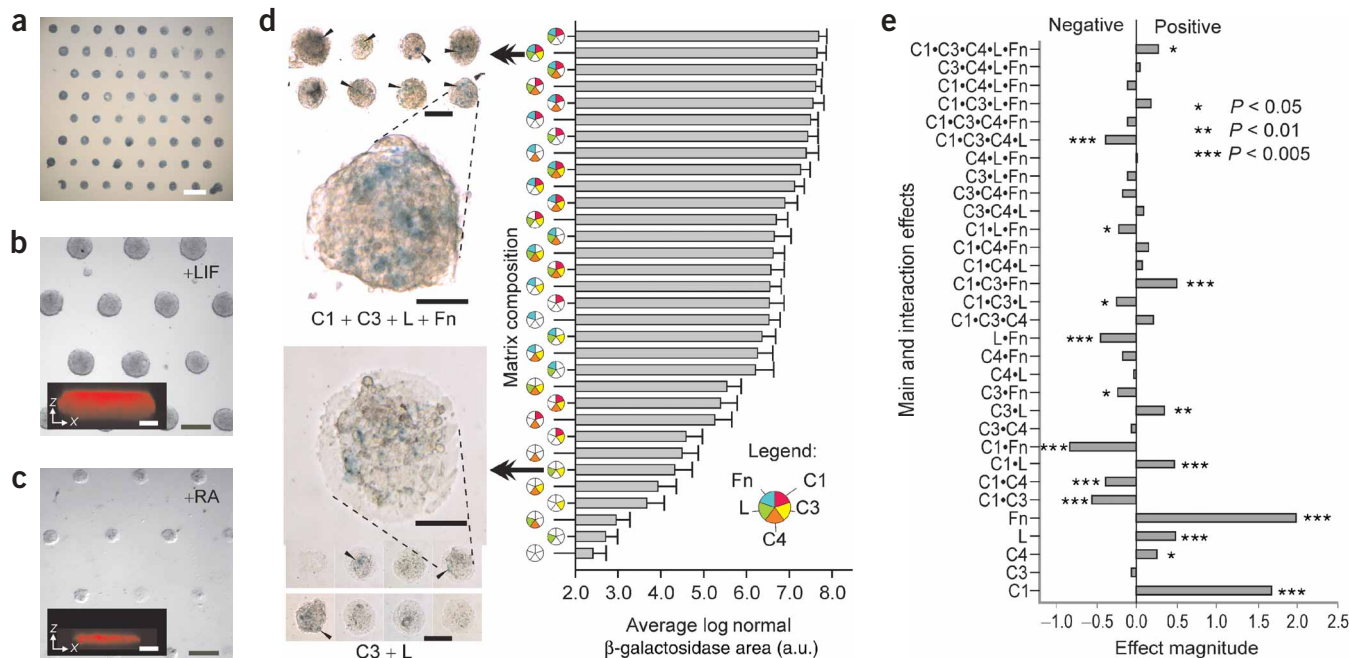


Figure 5 | I114 ES cells differentiate on ECM microarrays. (a) Bright-field alkaline phosphatase staining of day 1 ES cultures on ECM microarrays in 15% serum medium (scale bar, 1 mm). (b,c) Phase-contrast images of day 3 arrays cultured with LIF (b) and with RA (c). Cells cultured with LIF showed three-dimensional features (in b, inset x-z confocal section, $\sim 77 \mu\text{m}$ thickness). In contrast, RA-induced cells grew as a relatively thin sheet (in c, inset x-z section, $\sim 25 \mu\text{m}$ thickness). Scale bars, 250 μm (inset scale bars, 50 μm). (d) Bright-field micrograph of selected X-gal-stained ECM microarray conditions after 3 d of culture in RA. C1 + C3 + L + Fn (top left images) induced higher *Ankrd17* reporter activity (arrowheads) than was seen in cells cultured on C3 + L (bottom left images). Scale bars, 250 μm . Magnified views of reporter activity: scale bars, 50 μm . Bar graph: hierarchical depiction of 'blue' image area (pooled data from four microarrays) for each of the matrix mixtures. Error bars, s.e.m. ($n = 32$). The C1 + C3 + L + Fn culture condition induced ~ 27 -fold more β -galactosidase image area than the C3 + L cultures. (e) Results of 2^5 full factorial analysis on β -galactosidase positive 'blue' image area (four microarray data sets). The relative magnitude of main effects as well as 2-, 3-, 4- and 5-factor interactions are shown. C1, collagen I; C3, collagen III; C4, collagen IV; L, laminin; Fn, fibronectin.

hepatocytes is highest when the cells are cultured on collagen IV and lower when they are cultured on fibronectin and laminin^{27,28}. Notably, several 2-, 3- and 4-factor interactions were also identified as statistically significant ($P < 0.05$). The interactions of collagen I with laminin and of collagen III with laminin both had positive effects. However, each of these components individually produced a negative effect, suggesting a nonadditive interaction. Similarly, the interaction of collagen IV with fibronectin showed a negative effect, whereas individually these components displayed positive effects. These findings could be the subject of future investigations.

To investigate the feasibility of using matrix arrays to study stem cell differentiation, we cultured I114 mouse ES cells for up to 6 d in the presence of 1,000 U/ml leukemia inhibitory factor (LIF) or 10^{-6} M all-*trans* retinoic acid (RA). Day 1 cultures stained uniformly positive for alkaline phosphatase (Fig. 5a). Cells cultured with LIF for 3 d (Fig. 5b) grew as three-dimensional clusters that were reminiscent of embryoid bodies (EBs) with an average diameter $224 \pm 12 \mu\text{m}$ ($n = 14$). Confocal sectioning (Fig. 5b, inset) indicated that islands were $\sim 77 \mu\text{m}$ thick (possibly multi-layered). When cultured with RA, the cells grew as a relatively thin sheet $\sim 25 \mu\text{m}$ thick (Fig. 5c, inset). Notably, several matrix conditions in day 3 and 5 RA-induced cultures elicited a substantial increase of β -galactosidase reporter activity when stained with 5-bromo-4-chloro-3-indolyl- β -D-galactosidase (X-gal). For example, collagen I + collagen III + laminin + fibronectin collectively induced noticeably more reporter expression in all replicate islands

(Fig. 5d, top left images) than was seen in cells cultured on collagen III + laminin (Fig. 5d, bottom left images). Quantitative image analysis of 'blue' threshold area in day 3 RA-treated arrays illuminated further trends (Fig. 5d, bar graph). We note that nine of the ten highest signals were recorded from cells on matrices that contained collagen I, and four of the top five signals came from ECM conditions including both collagen I and fibronectin. We also found that the lowest eleven signals were detected on matrices that lacked fibronectin, and matrices that lacked both collagen I and fibronectin produced the lowest seven β -galactosidase signals. A 2^5 full factorial analysis on data from four arrays also indicated that fibronectin and collagen I had strong positive effects on β -galactosidase reporter expression (Fig. 5e). Again, several potentially counterintuitive interaction effects were identified (for example, collagen I + collagen IV and collagen I + fibronectin).

DISCUSSION

Fabrication of an ECM microarray for cell culture required optimization of the deposition method, printing buffer, microarray surface and cell culture conditions. We chose a contact style arrayer using pins that deposited 1–2 nl of material per $\sim 150 \mu\text{m}$ diameter spot, which is large enough to accommodate more than 20 cells. The spotting buffer also had considerable influence on microarray quality, and required reformulation to accommodate ECM proteins: an acidic buffer to inhibit collagen polymerization,

5 mM EDTA to prevent laminin polymerization²⁹, Triton X-100 to reduce surface tension and glycerol to slow evaporation and increase the volume of material deposited (data not shown). When using this buffer and cleaning the pins by dipping them in dimethyl sulfoxide (DMSO) between wells and subjecting them to daily sonication, we observed no defects during six consecutive printing runs (>100 arrays produced).

The choice of microarray surface is key to maintaining spatially separated cellular islands. We chose a surface that allowed ECM molecules to be stored locally in a hydrated environment, yet resisted adsorption of serum proteins. The nonfouling nature of acrylamide prevents cell migration over relatively long periods of time (>28 d) in comparison to other cell patterning techniques that use agarose, Pluronic compounds, serum albumin or polyethylene glycol (<7 d)³⁰. Dehydrated polyacrylamide substrates are thought to swell during spotting and retain proteins through hydrophobic interactions³¹. Although here we report culture only up to 7 d, we note that when our substrates failed, it was due to gel detachment from the glass slide rather than cell migration. This failure mode could potentially be improved by ensuring that the glass surface is densely hydroxylated before silanization, or by using a highly porous glass substrate or alternate silane coupling agents^{32–35}.

Cell culture presents additional demands on the ECM microarray concept. A minimum surface density of integrin ligands is required for cell attachment and spreading³⁶ and is estimated to be as low as 1 ng/cm² for hepatocyte cells on laminin, fibronectin, collagen I and collagen IV³⁷. In our hands, hepatocytes attached to hydrogel spots in which ~25 pg of protein was initially deposited (<130 ng/cm²), putting it within a reasonable range. The maximum density of ECM molecules is dependent on several factors including the concentration of stock solution, the solubility of ECM proteins, the porosity of the polyacrylamide gel and the mode of deposition (pin or piezoelectric).

Our interest in the liver inspired the choice of ECM molecules found in the hepatic microenvironment, the use of primary cells and a fetal liver-specific reporter ES cell line. The liver has heterogeneous staining for collagen I, collagen III, collagen IV, laminin and fibronectin^{38,39}. Hepatocytes display integrins β 1, β 2, α 1, α 2, α 5 and the nonintegrin fibronectin receptor Agp110 *in vivo*^{38,40}. Cultured rat hepatocytes display integrins α 1, α 3, α 5, β 1 and α 6 β 1, and their expression is modulated by the culture conditions⁴¹. In our experiments, we emphasize that only the initial matrix composition was specified; however, interaction with ECM is well known to modulate matrix metalloproteinase expression⁴², integrin activity⁴³ and matrix expression^{27,44}, making it a key parameter in investigating optimal culture environments.

Interactions between ECM and growth factors, which can be positive or negative, have been reported in several contexts⁴⁵. In addition to the well-described crosstalk between integrin and growth factor signaling⁴⁶, crosstalk exists among matrix molecules. For example, it has been previously reported that collagen-induced release of IL-1 through binding integrin α 7 β 1 in human blood mononuclear cells is potentiated by fibronectin binding to α 5 β 1^{43,47}. Similarly, endothelial cell attachment to fibronectin via α 5 β 1 integrin reportedly potentiates α v β 3-mediated migration on vitronectin⁴⁸. In this context, our results with hepatocytes suggest that integrin crosstalk may explain the apparent antagonistic interactions between collagen III and laminin, and collagen IV and fibronectin,

a hypothesis that is testable by scaling-up the appropriate culture conditions so that conventional methods can be used³.

Embryonic stem cells are a potential source of differentiated cells that could be used in cell therapy, drug discovery and basic research. Current methods for differentiating ES cells *in vitro* are generally inefficient (<1%) for generating specific lineages, and rely on the use of heterogeneous cell aggregates called embryoid bodies. Exceptions to this generalization are a few rare reports of efficient monolayer culture methods, underscoring the importance of a tightly regulated environment for efficient lineage-specific differentiation^{1,49,50}. Whereas most studies focus on growth factors, the importance of ECM in developmental processes has increasingly been recognized. *In vitro*, undifferentiated mouse ES cells express integrins α 6, β 1, β 4, β 5, laminin receptor 1 and dystroglycan^{51–53}, and are thus poised to receive signals from ECM. Given that stem cell differentiation has historically been a largely empirical field, a parallelized culture platform could be of benefit. A potential difficulty that could result from miniaturization is that low differentiation efficiency would not yield a detectable level of cells expressing the desired lineage markers, necessitating monitoring of more ubiquitous cellular constituents such as actin and keratin⁴.

We chose to explore the feasibility of using ECM protein microarrays to study ES differentiation in the context of the liver. Preliminary evidence exists for the *in vitro* differentiation of mouse ES cells into hepatic tissue^{54–57}. *In vitro* differentiation of mouse I114 reporter ES cells as embryoid bodies induces reporter expression that coincides with endodermal gene upregulation and colocalization with α -fetoprotein and albumin protein^{25,26,58}. As such, it can potentially serve as a tool to study early hepatic specification *in vitro*. Culturing ES cells as three-dimensional aggregates greatly improves the frequency of differentiation to somatic lineages; however, embryoid bodies are seldom uniform in size. We observed uniform, spatially confined, three-dimensional growth of ES cells cultured on ECM microarrays with LIF, which we propose is a result of proliferation on a confined domain. In contrast, culturing with RA resulted in a noticeable flattening of the cellular island morphology, probably owing to induction of differentiation, a reduction in proliferation, and therefore less expansion in the *z*-direction. From image analysis, we estimated <1% reporter activity in day 9 EBs⁵⁸ and even less in monolayer cultures. In contrast, our day 3 RA-induced microcultures exhibited up to $16.8 \pm 5.5\%$ ($n = 8$) of the island area that showed reporter activity when cultured on optimal ECM microenvironments. Moreover, we detected an approximate 140-fold difference in β -galactosidase signal from the least efficient condition (laminin only) to the most efficient (laminin + collagen I + fibronectin). In analyzing these results, it is important to bear in mind that only the initial, underlying matrix composition was experimentally specified. Alterations that resulted from this experimental variable may be due to the influence on proliferation, differentiation, matrix remodeling or cell-cell interactions. Further investigation of how complex ECM enhances reporter activity may provide valuable insight on how to drive the *in vitro* differentiation more efficiently.

The diversity of biological niches mandates a systematic approach to investigating optimal cell culture environments. Miniaturized arrays of living cells, like DNA microarrays, offer the potential for a more global picture of the role of soluble and insoluble cues on cell fate and function. We have described here a robust method to create cell arrays using only a DNA spotter and

off-the-shelf chemicals. Culturing primary hepatocytes and mouse ES cells on combinatorial mixtures of ECM yielded insights into the role of the microenvironment using 1,000 times less protein than conventional methods would require. This method is amenable to depositing almost any insoluble or soluble cue, such as polysaccharides, proteoglycans, glycosaminoglycans, membrane bound proteins and tethered growth factors or peptide signaling motifs. It can also be easily adapted to exploit lineage-specific fluorescent reporter strategies, cocultivate epithelia and stroma, and, when combined with soluble factors, screen the effects of growth factors or small molecules in conjunction with underlying matrix^{2,59}.

METHODS

ECM microarray fabrication. The microarray substrate was a custom-fabricated acrylamide gel pad slide, similar to the Hydrogel slide (Perkin Elmer) and those described elsewhere^{35,60}. To summarize, glass slides were modified with 3-(trimethoxysilyl)propyl methacrylate (Sigma) to present methacrylate groups that bond the gel to the glass. A thin (~80 µm) polyacrylamide gel pad was created by floating an untreated 22 × 22 mm #1 coverslip on a 40 µl drop of prepolymer solution and exposing to UV at 1.5 mW/cm² for 10 min (Glo-Mark Systems, Inc.). The prepolymer solution consisted of 9.5% acrylamide, 0.5% bis and 20 mg/ml 1-[4-(2-hydroxyethoxy)-phenyl]-2-hydroxy-2-methyl-1-propane-1-one (Irgacure 2959, Ciba Specialty Chemicals; dissolved initially in methanol at 200 mg/ml). After carefully removing the coverslip, the slides were soaked in deionized H₂O (dH₂O) for 48 h and dehydrated on a hot plate at 40 °C. The printing buffer consisted of 100 mM acetate, 5 mM EDTA, 20% glycerol and 0.25% Triton X-100, and it was adjusted to pH 5.0 to inhibit protein polymerization. For ECM arrays, stock solutions of rat collagen I (ref. 8), human collagen III, mouse collagen IV, human fibronectin (Becton Dickinson) and mouse laminin (Sigma) were suspended at 500 µg/ml in the printing buffer. ECM protein solutions were then mixed in 32 combinations in a 384-well plate. Eight individual spots of each protein mixture were deposited with a 500 µm pitch on the acrylamide gel pad using a SpotArray 24 (Perkin Elmer) equipped with Stealth SMP 3.0 split pins (Telechem). The pins were cleaned by sonication in 5% Micro Cleaning Solution (Telechem) and dH₂O immediately before use. Between each sample in the source plate, the pins were dipped in a 50% DMSO and water solution, washed for 25 s with dH₂O and dried. Twenty ECM microarrays could be produced simultaneously in this manner in 1 h. A silicone well isolator (Grace Biolabs) was adhered around the gel pad using Silicone II sealant (General Electric) to define the cell culture area. The protein arrays with gaskets were incubated at 4 °C in a humidified environment for ~16 h and rinsed in phosphate-buffered saline (PBS) before use.

Cellular function. Images of the 9 mm × 9 mm array were acquired at 10× magnification as a series of 154 images on a Nikon inverted microscope equipped with a motorized stage (Ludl Electronic Products Ltd.). The images were montaged using Metamorph 6.2r3 software (Universal Imaging Corp.). Hepatocyte arrays were fixed on days 1 and 7 in 4% paraformaldehyde and stained for intracellular albumin using a rabbit anti-rat albumin antibody (Cappel) and a goat anti-rabbit IgG-Alexa 633 secondary antibody (Molecular Probes). Arrays were mounted in Slowfade

Light (Molecular Probes) and imaged using 3 s exposures for each frame (CoolSnap HQ, Photometrics).

I114 ES cell reporter expression was assessed on days 3 and 5. Cell arrays were fixed for 20 min in 0.5% glutaraldehyde and stained in 0.1% X-gal in a Tris buffer (pH 7.5) overnight at 37 °C. Montaged images of each array were acquired in bright field. B-galactosidase image area was quantified by color thresholding using Metamorph software.

Indirect immunofluorescence, cell culture, cell function and data analysis. See **Supplementary Methods** online.

Note: Supplementary information is available on the Nature Methods website.

ACKNOWLEDGMENTS

We would like to thank L. Forrester (University of Edinburgh) for providing the I114 cell line, C. Largent (Cel Associates) and D. Schabacker (Argonne) for useful discussions about acrylamide-gel pad fabrication, T. Martinsky (Telechem) for printing parameters, J. Norwich (S. Chien Lab), R. Agustin (imaging, J. Price Lab), J. Emond and R. Lieber (biostatistics), S. Khetani (cell patterning), J. Felix (hepatocyte isolation) and O. Tran. Funding was generously provided by the US National Institutes of Health, the National Institute of Diabetes and Digestive and Kidney Diseases, the National Science Foundation's Faculty Early Career Development (CAREER) Program and the David and Lucile Packard Foundation.

COMPETING INTERESTS STATEMENT

The authors declare that they have no competing financial interests.

Received 2 December; accepted 21 December 2004

Published online at <http://www.nature.com/naturemethods/>

- Ding, S. *et al.* Synthetic small molecules that control stem cell fate. *Proc. Natl. Acad. Sci. USA* **100**, 7632–7637 (2003).
- Revzin, A. *et al.* Designing a hepatocellular microenvironment with protein microarraying and poly(ethylene glycol) photolithography. *Langmuir* **20**, 2999–3005 (2004).
- Prudhomme, W., Daley, G.Q., Zandstra, P. & Luffenburger, D.A. Multivariate proteomic analysis of murine embryonic stem cell self-renewal versus differentiation signaling. *Proc. Natl. Acad. Sci. USA* **101**, 2900–2905 (2004).
- Anderson, D.G., Levenberg, S. & Langer, R. Nanoliter-scale synthesis of arrayed biomaterials and application to human embryonic stem cells. *Nat. Biotechnol.* **22**, 863–866 (2004).
- Meredith, J.E. Jr. *et al.* The regulation of growth and intracellular signaling by integrins. *Endocr. Rev.* **17**, 207–220 (1996).
- Comoglio, P.M., Boccaccio, C. & Trusolino, L. Interactions between growth factor receptors and adhesion molecules: breaking the rules. *Curr. Opin. Cell Biol.* **15**, 565–571 (2003).
- Hall, H.G., Farson, D.A. & Bissell, M.J. Lumen formation by epithelial cell lines in response to collagen overlay: a morphogenetic model in culture. *Proc. Natl. Acad. Sci. USA* **79**, 4672–4676 (1982).
- Dunn, J.C., Yarmush, M.L., Koebe, H.G. & Tompkins, R.G. Hepatocyte function and extracellular matrix geometry: long-term culture in a sandwich configuration. *FASEB J.* **3**, 174–177 (1989).
- Cukierman, E., Pankov, R., Stevens, D.R. & Yamada, K.M. Taking cell-matrix adhesions to the third dimension. *Science* **294**, 1708–1712 (2001).
- Baatout, S. Endothelial differentiation using Matrigel (review). *Anticancer Res.* **17**, 451–455 (1997).
- Lindberg, K. & Badylak, S.F. Porcine small intestinal submucosa (SIS): a bioscaffold supporting in vitro primary human epidermal cell differentiation and synthesis of basement membrane proteins. *Burns* **27**, 254–266 (2001).
- Lin, P., Chan, W.C.W., Badylak, S. & Bhatia, S. Assessing the function of porcine liver-derived matrix: applications to hepatic tissue engineering. *Tissue Eng.* **10**, 1046–1053 (2004).
- Mann, B.K., Gobin, A.S., Tsai, A.T., Schmedlen, R.H. & West, J.L. Smooth muscle cell growth in photopolymerized hydrogels with cell adhesive and proteolytically degradable domains: synthetic ECM analogs for tissue engineering. *Biomaterials* **22**, 3045–3051 (2001).
- Hern, D.L. & Hubbell, J.A. Incorporation of adhesion peptides into nonadhesive hydrogels useful for tissue resurfacing. *J. Biomed. Mater. Res.* **39**, 266–276 (1998).
- Anseth, K.S., Shastri, V.R. & Langer, R. Photopolymerizable degradable polyamides with osteocompatibility. *Nat. Biotechnol.* **17**, 156–159 (1999).

16. Singhvi, R. *et al.* Engineering cell-shape and function. *Science* **264**, 696–698 (1994).
17. Chen, C.S., Mrksich, M., Huang, S., Whitesides, G.M. & Ingber, D.E. Geometric control of cell life and death. *Science* **276**, 1425–1428 (1997).
18. Bhatia, S.N., Yarmush, M.L. & Toner, M. Controlling cell interactions by micropatterning in co-cultures: hepatocytes and 3T3 fibroblasts. *J. Biomed. Mater. Res.* **34**, 189–199 (1997).
19. Kane, R.S., Takayama, S., Ostuni, E., Ingber, D.E. & Whitesides, G.M. Patterning proteins and cells using soft lithography. *Biomaterials* **20**, 2363–2376 (1999).
20. MacBeath, G. & Schreiber, S.L. Printing proteins as microarrays for high-throughput function determination. *Science* **289**, 1760–1763 (2000).
21. Houseman, B.T. & Mrksich, M. Carbohydrate arrays for the evaluation of protein binding and enzymatic modification. *Chem. Biol.* **9**, 443–454 (2002).
22. Falsey, J.R., Renil, M., Park, S., Li, S.J. & Lam, K.S. Peptide and small molecule microarray for high throughput cell adhesion and functional assays. *Bioconj. Chem.* **12**, 346–353 (2001).
23. Ziauddin, J. & Sabatini, D.M. Microarrays of cells expressing defined cDNAs. *Nature* **411**, 107–110 (2001).
24. Mousses, S. *et al.* RNAi microarray analysis in cultured mammalian cells. *Genome Res.* **13**, 2341–2347 (2003).
25. Forrester, L.M. *et al.* An induction gene trap screen in embryonic stem cells: Identification of genes that respond to retinoic acid *in vitro*. *Proc. Natl. Acad. Sci. USA* **93**, 1677–1682 (1996).
26. Watt, A.J. *et al.* A gene trap integration provides an early *in situ* marker for hepatic specification of the foregut endoderm. *Mech. Dev.* **100**, 205–215 (2001).
27. Sudhakaran, P.R., Stamatoglou, S.C. & Hughes, R.C. Modulation of protein synthesis and secretion by substratum in primary cultures of rat hepatocytes. *Exp. Cell Res.* **167**, 505–516 (1986).
28. Hughes, R.C. & Stamatoglou, S.C. Adhesive interactions and the metabolic activity of hepatocytes. *J. Cell Sci. Suppl.* **8**, 273–291 (1987).
29. Freire, E. & Coelho-Sampaio, T. Self-assembly of laminin induced by acidic pH. *J. Biol. Chem.* **275**, 817–822 (2000).
30. Nelson, C.M., Raghavan, S., Tan, J.L. & Chen, C.S. Degradation of micropatterned surfaces by cell-dependent and -independent processes. *Langmuir* **19**, 1493–1499 (2003).
31. Angenendt, P., Glokler, J., Murphy, D., Lehrach, H. & Cahill, D.J. Toward optimized antibody microarrays: a comparison of current microarray support materials. *Anal. Biochem.* **309**, 253–260 (2002).
32. Revzin, A. *et al.* Fabrication of poly(ethylene glycol) hydrogel microstructures using photolithography. *Langmuir* **17**, 5440–5447 (2001).
33. Koh, W.G., Revzin, A. & Pishko, M.V. Poly(ethylene glycol) hydrogel microstructures encapsulating living cells. *Langmuir* **18**, 2459–2462 (2002).
34. Kim, C.O., Hong, S.-Y., Kim, M., Park, S.-M. & Park, J.W. Modification of indium-tin oxide (ITO) glass with aziridine provides a surface of high amine density. *J. Colloid Interface Sci.* **277**, 499–504 (2004).
35. Timofeev, E., Kochetkova, S.V., Mirzabekov, A.D. & Florentiev, V.L. Regioselective immobilization of short oligonucleotides to acrylic copolymer gels. *Nucleic Acids Res.* **24**, 3142–3148 (1996).
36. Massia, S.P. & Hubbell, J.A. An RGD spacing of 440 nm is sufficient for integrin $\alpha V \beta 3$ -mediated fibroblast spreading and 140 nm for focal contact and stress fiber formation. *J. Cell Biol.* **114**, 1089–1100 (1991).
37. Mooney, D. *et al.* Switching from differentiation to growth in hepatocytes: control by extracellular matrix. *J. Cell Physiol.* **151**, 497–505 (1992).
38. Pinkse, G.G. *et al.* Hepatocyte survival depends on $\beta 1$ -integrin-mediated attachment of hepatocytes to hepatic extracellular matrix. *Liver Int.* **24**, 218–226 (2004).
39. Martinez-Hernandez, A. & Amenta, P.S. The hepatic extracellular matrix. I. Components and distribution in normal liver. *Virchows Arch. A Pathol. Anat. Histopathol.* **423**, 1–11 (1993).
40. Stamatoglou, S.C., Enrich, C., Manson, M.M. & Hughes, R.C. Temporal changes in the expression and distribution of adhesion molecules during liver development and regeneration. *J. Cell Biol.* **116**, 1507–1515 (1992).
41. Liu Tsang, V. *Three-dimensional photopatterning of hydrogels containing living cells for hepatic tissue engineering*. Ph.D. dissertation, University of California San Diego, La Jolla (2004).
42. Werb, Z., Tremble, P.M., Behrendtsen, O., Crowley, E. & Damsky, C.H. Signal transduction through the fibronectin receptor induces collagenase and stromelysin gene expression. *J. Cell Biol.* **109**, 877–889 (1989).
43. Pacifici, R. *et al.* Ligand binding to monocyte $\alpha 5 \beta 1$ integrin activates the $\alpha 2 \beta 1$ receptor via the $\alpha 5$ subunit cytoplasmic domain and protein kinase C. *J. Immunol.* **153**, 2222–2233 (1994).
44. Diegelmann, R.F., Guzelian, P.S., Gay, R. & Gay, S. Collagen formation by the hepatocyte in primary monolayer culture and *in vivo*. *Science* **219**, 1343–1345 (1983).
45. Fashena, S.J. & Thomas, S.M. Signalling by adhesion receptors. *Nat. Cell Biol.* **2**, E225–E229 (2000).
46. Schwartz, M.A. & Ginsberg, M.H. Networks and crosstalk: integrin signalling spreads. *Nat. Cell Biol.* **4**, E65–E68 (2002).
47. Pacifici, R. *et al.* Collagen-induced release of interleukin 1 from human blood mononuclear cells. Potentiation by fibronectin binding to the $\alpha 5 \beta 1$ integrin. *J. Clin. Invest.* **89**, 61–67 (1992).
48. Kim, S., Harris, M. & Varner, J.A. Regulation of integrin $\alpha \beta 3$ -mediated endothelial cell migration and angiogenesis by integrin $\alpha 5 \beta 1$ and protein kinase A. *J. Biol. Chem.* **275**, 33920–33928 (2000).
49. Rathjen, J. *et al.* Directed differentiation of pluripotent cells to neural lineages: homogeneous formation and differentiation of a neuroectoderm population. *Development* **129**, 2649–2661 (2002).
50. Ying, Q.L., Stavridis, M., Griffiths, D., Li, M. & Smith, A. Conversion of embryonic stem cells into neuroectodermal precursors in adherent monoculture. *Nat. Biotechnol.* **21**, 183–186 (2003).
51. Ivanova, N.B. *et al.* A stem cell molecular signature. *Science* **298**, 601–604 (2002).
52. Ramalho-Santos, M., Yoon, S., Matsuzaki, Y., Mulligan, R.C. & Melton, D.A. “Stemness”: transcriptional profiling of embryonic and adult stem cells. *Science* **298**, 597–600 (2002).
53. Kelly, D.L. & Rizzino, A. DNA microarray analyses of genes regulated during the differentiation of embryonic stem cells. *Mol. Reprod. Dev.* **56**, 113–123 (2000).
54. Hamazaki, T. *et al.* Hepatic maturation in differentiating embryonic stem cells *in vitro*. *FEBS Lett.* **497**, 15–19 (2001).
55. Yamada, T. *et al.* *In vitro* differentiation of embryonic stem cells into hepatocyte-like cells identified by cellular uptake of indocyanine green. *Stem Cells* **20**, 146–154 (2002).
56. Chinzei, R. *et al.* Embryoid-body cells derived from a mouse embryonic stem cell line show differentiation into functional hepatocytes. *Hepatology* **36**, 22–29 (2002).
57. Ishizaka, S. *et al.* Development of hepatocytes from ES cells after transfection with the HNF-3 β gene. *FASEB J.* **16**, 1444–1446 (2002).
58. Jones, E.A., Tosh, D., Wilson, D.I., Lindsay, S. & Forrester, L.M. Hepatic differentiation of murine embryonic stem cells. *Exp. Cell Res.* **272**, 15–22 (2002).
59. Subramanian, S. & Srienc, F. Quantitative analysis of transient gene expression in mammalian cells using the green fluorescent protein. *J. Biotechnol.* **49**, 137–151 (1996).
60. Arenkov, P. *et al.* Protein microchips: use for immunoassay and enzymatic reactions. *Anal. Biochem.* **278**, 123–131 (2000).